

Subsea Oil Spill Risk Management Based on Sensor Networks

Gianluca Tabella^{a,*}, Nicola Paltrinieri^b, Valerio Cozzani^c, Pierluigi Salvo Rossi^a

^aDepartment of Electronic Systems, NTNU Norwegian University of Science and Technology, Norway

^bDepartment of Mechanical and Industrial Engineering, NTNU Norwegian University of Science and Technology, Norway

^cDepartment of Civil, Chemical, Environmental, and Materials Engineering, University of Bologna, Italy

gianluca.tabella@ntnu.no

The use of Wireless Sensor Networks (WSNs) in support of Dynamic Risk Assessment regarding oil spills still lacks a proper integration. WSNs enable prompt responses to such emergencies through an appropriate inspection, thus avoiding possible larger disasters. This work proposes a methodology for the setup of a WSN as a Leak Detection System in which a Fusion Center collects sensors' binary decisions and provides a more reliable decision about the presence/absence of a leak. The detection rules are based on statistical signal processing techniques, and the choice of the optimal thresholds is made through the optimization of three objective functions tailored to the Oil&Gas industry. Detection performances are assessed in terms of the Receiver Operating Characteristic (ROC) curve. The case study is the Goliat FPSO, a production platform located in the Barents Sea, and related requirements dictated by Norwegian authorities to prevent oil spills. The considered WSN monitors the subsea manifolds through passive acoustic sensors.

1. Introduction

Oil spills are known to cause a highly negative impact on the safety of offshore workers, the environment, and productivity. The early detection of a spill is crucial to limit its potential consequences. A Leak Detection System (LDS) is reliable if it can provide a high rate of correct detections ensuring a limited rate of false alarms, thus avoiding unnecessary production shutdowns and costly Remotely Operated Vehicles (ROV) inspections. Different technologies, among which the use of passive acoustic sensors, are nowadays available and are used to monitor the external underwater environment and the process conditions (Adegboye et al., 2019; Baroudi et al., 2019). Passive acoustic sensors have shown a high level of accuracy enabling the possibility to localize the spill source. This can be done without the need to install the sensors near the leaking component (which is a limitation of many other LDSs). Also, this technology can detect all hydrocarbon fluids. Acoustic sensors are easy to install and are appropriate for retrofitting. These properties make this LDS among the most used. The importance of a reliable LDS creates the need for a framework that integrates it into the Dynamic Risk Assessment (DRA). This is possible as the use of a distributed Wireless Sensor Network (WSN) can provide real-time monitoring of the subsea environment increasing the level of knowledge on the system allowing a more accurate DRA (Paltrinieri et al., 2014, 2019a). So far, the application of WSNs in the Oil&Gas industry has only been introduced (Paltrinieri et al., 2019b). This work gives a methodology for the setup of passive acoustic sensors in a WSN used for monitoring subsea templates and discusses its performances.

2. Signal Model

The WSN aims at detecting possible oil spills, so the problem is formalized as a binary hypothesis testing with the null hypothesis H_0 corresponding to a non-spill scenario, and the alternative hypothesis H_1 corresponding to a spill scenario. For the generic k th sensor, the two following different signal models are assumed for each hypothesis:

$$\begin{cases} H_1: & y_k = \xi \cdot AAF(\mathbf{x}_k, \mathbf{x}_T) + w_k \\ H_0: & y_k = w_k \end{cases} \Rightarrow \begin{cases} H_1: & y_k \sim \mathcal{N}(0, AAF^2(\mathbf{x}_k, \mathbf{x}_T) \cdot \sigma_s^2 + \sigma_w^2) \\ H_0: & y_k \sim \mathcal{N}(0, \sigma_w^2) \end{cases} \quad (1)$$

where:

- y_k is the signal (sound pressure) received at the k th sensor where $k = 1, 2, \dots, K$;
- $\xi \sim \mathcal{N}(0, \sigma_s^2)$ is a Gaussian random variable representing the emitted signal caused by the spill;
- $w_k \sim \mathcal{N}(0, \sigma_w^2)$ is Additive White Gaussian Noise having the same power σ_w^2 for any sensor;
- $AAF(\mathbf{x}_k, \mathbf{x}_T)$ is the Amplitude Attenuation Function (AAF) which only depends on the distance between the position \mathbf{x}_k (k th sensor position) and \mathbf{x}_T (leak position).

The AAF is treated deterministically and represents the loss of the acoustic intensity level and accounts for seawater absorption and geometrical spreading (Stojanovic, 2006):

$$10 \log AAF^2(\mathbf{x}_k, \mathbf{x}_T) = -\alpha \cdot 10^{-3} (\|\mathbf{x}_k - \mathbf{x}_T\| - \ell_{\text{ref}}) - k_{\text{sc}} \cdot 10 \log \left(\frac{\|\mathbf{x}_k - \mathbf{x}_T\|}{\ell_{\text{ref}}} \right) \quad (2)$$

From which, the AAF can be obtained:

$$AAF(\mathbf{x}_k, \mathbf{x}_T) = \sqrt{\left(\frac{\ell_{\text{ref}}}{\|\mathbf{x}_k - \mathbf{x}_T\|} \right)^{k_{\text{sc}}} 10^{\left[\frac{\alpha}{10^4} (\ell_{\text{ref}} - \|\mathbf{x}_k - \mathbf{x}_T\|) \right]}} \quad (3)$$

where α is the seawater absorption coefficient in dB/km, $\|\mathbf{x}_k - \mathbf{x}_T\|$ and ℓ_{ref} (reference length) are in meters, and k_{sc} is the spreading coefficient. The absorption coefficient α is obtained using the Francois & Garrison equation (Francois and Garrison, 1982a, 1982b). The speed of sound (required by Francois & Garrison) is obtained using the updated Chen & Millero equation (Wong and Zhu, 1995).

3. Wireless Sensor Network Model

The modeled WSN is made of K passive acoustic sensors monitoring the external environment (as shown in Figure 1). The k th sensor, with a given sampling frequency, senses the received signal amplitude y_k and sends to a Fusion Center (FC) its binary local decision d_k on whether the sensed amplitude is caused by a spill. The choice of local binary decision is due to the energy constraints imposed by the use of a WSN (Shoari et al., 2016), such constraint will also reduce operating costs as only one bit is transmitted when a spill is detected. Finally, the FC takes a global decision \hat{H} on the occurrence of the spill based on the received d_k 's.

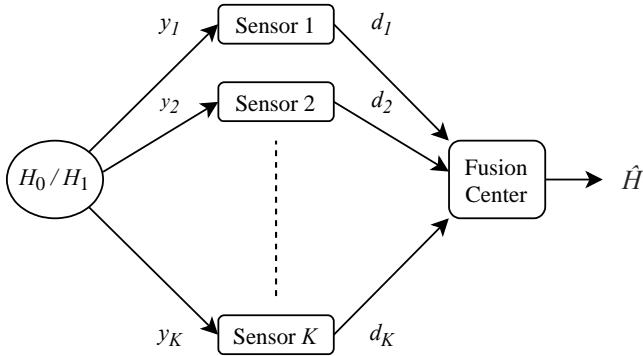


Figure 1: Wireless Sensor Network Model

4. Detection Rules

Each sensor performs an Energy Test, which is Uniformly Most Powerful for this application, where the signal energy y_k^2 is compared to a threshold λ_k to assess its decision (Ciunzono and Salvo Rossi, 2017):

$$d_k = \begin{cases} 1, & y_k^2 \geq \lambda_k \\ 0, & y_k^2 < \lambda_k \end{cases} \quad (4)$$

As the statistics of the received signal is known, the Local Probability of Detection ($P_{d,k}$) and Local Probability of False Alarm ($P_{f,k}$) for the k th sensor can be defined as follows:

$$P_{d,k} = \Pr(y_k^2 \geq \lambda_k | H_1) = 2Q \left(\sqrt{\frac{\lambda_k}{AAF^2(\mathbf{x}_k, \mathbf{x}_T) \cdot \sigma_s^2 + \sigma_w^2}} \right) \quad (5)$$

$$P_{f,k} = \Pr(y_k^2 \geq \lambda_k | H_0) = 2Q \left(\sqrt{\frac{\lambda_k}{\sigma_w^2}} \right) \quad (6)$$

where $Q(x)$ is the complementary cumulative distribution function of the standard normal random variable:

$$Q(x) = \frac{1}{2\pi} \int_x^\infty \exp\left(-\frac{t^2}{2}\right) dt \quad (7)$$

The proposed method assumes the Signal-to-Noise Ratio $SNR_T = \sigma_s^2 / \sigma_w^2$ at ℓ_{ref} from the source to be known. The Counting Rule is used as Fusion Rule by the FC because of its simplicity which suits the constraint of low processing costs. This rule uses the local decisions d_k as an input and has the following form:

$$\hat{H} = \begin{cases} H_1, & \sum_{k=1}^K d_k \geq \Lambda \\ H_0, & \sum_{k=1}^K d_k < \Lambda \end{cases} \quad (8)$$

This indicates that the FC counts the number of sensors detecting the spill and compares it to a threshold Λ . In case the sum is equal or higher than the threshold, the FC sends an alarm.

5. Threshold Selection

Three different optimality criteria based on the Receiver Operating Characteristic (ROC) curve will be analyzed (Liu, 2012):

- Youden Index (J):

$$\lambda^* = \arg \max_{\lambda} J(\lambda) = \arg \max_{\lambda} \{P_d(\lambda) - P_f(\lambda)\} \quad (9)$$

- Closest-to-(0,1) (ER):

$$\lambda^* = \arg \min_{\lambda} ER(\lambda) = \arg \min_{\lambda} \sqrt{(1 - P_d(\lambda))^2 + P_f(\lambda)^2} \quad (10)$$

- Concordance Probability (CZ):

$$\lambda^* = \arg \max_{\lambda} CZ(\lambda) = \arg \max_{\lambda} \{P_d(\lambda) \cdot (1 - P_f(\lambda))\} \quad (11)$$

These definitions are applicable both for the sensors and the FC with the appropriate substitutions (λ is λ_k and Λ ; P_d is $P_{d,k}$ and Q_d ; P_f is $P_{f,k}$ and Q_f ; λ^* is λ_k^* and Λ^*). The selection of the optimal threshold λ_k^* for the k th sensor is carried out through a grid search where one optimal value is found for each one of the criteria. More specifically, the metrics in the optimality criteria are computed referring to average performances with respect to the hotspot positions \mathbf{h}_m , where $m = 1, 2, \dots, M$. This is necessary as the Probabilities of Detection (both local and global) depend on the leak position. The hotspots are those components of the subsea production system that, in case of failure, would be the source of a spill. Also, it is assumed that the selected hotspots have the same failure rate and their spills cause signals having the same power σ_s^2 . Therefore:

$$\begin{cases} \overline{P_{d,k}} = \frac{1}{M} \sum_{m=1}^M P_{d,k,m} \\ \overline{P_{f,k}} = P_{f,k} \end{cases} \xrightarrow{\text{optimize objective function}} \lambda_k^* \quad (12)$$

where, for the k th sensor, λ_k^* is the chosen local threshold (using one of the criteria), $\overline{P_{d,k}}$ and $\overline{P_{f,k}}$ are its average performances and $P_{d,k,m}$ is $P_{d,k}$ when the leak source is the m th hotspot by using $AAF(\mathbf{x}_k, \mathbf{h}_m)$.

The choice of the optimal threshold at the FC follows the local threshold choice and uses the same procedure:

$$\begin{cases} \overline{Q_d} = \frac{1}{M} \sum_{m=1}^M Q_{d,m} \\ \overline{Q_f} = Q_f \end{cases} \xrightarrow{\text{optimize objective function}} \Lambda^* \quad (13)$$

where Λ^* is the chosen global threshold. $Q_d = \Pr(\hat{H} = H_1 | H_1)$ and $Q_f = \Pr(\hat{H} = H_1 | H_0)$ are the values of Global Probability of Detection and Global Probability of False Alarm, where m means that the m th hotspot is

modeled as the leak source, and the bar denotes the average probability. $Q_{d,m}$ and Q_f are obtained via Monte Carlo Simulation requiring the simulation of the local decisions using the previously chosen local thresholds.

6. Case Study – Goliat FPSO

The Goliat FPSO is an offshore platform located in the Norwegian Barents Sea equipped with a multi-template Subsea Production System. Each template can host up to four wellheads and the manifold. The latter is monitored by three passive acoustic sensors to detect the presence of an oil spill (Bjørnbom, 2011; Røsby, 2011). For an overview of the subsea equipment, the reader could refer to the specific literature (Bai and Bai, 2012).

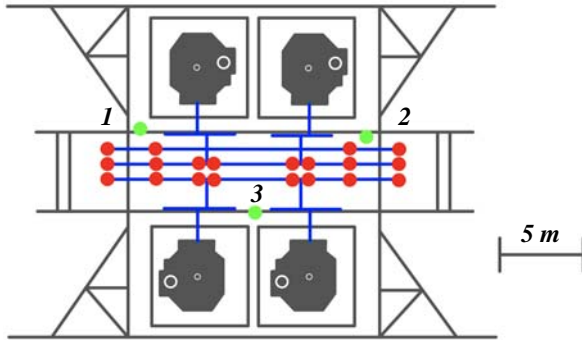


Figure 2: Scheme of Goliat's subsea template: the grey elements are the structure and the Christmas Trees, the blue lines are the main streamlines, the green dots are the sensors, and the red dots are the hotspots

20 hotspots (connections and valves) were recognized in the manifold. Hotspots and sensors are assumed to be at the same height. The following parameters are used for this case study:

Table 1: Parameters used to simulate the spill's sound emission and its Amplitude Attenuation Function

Parameter	Value	Note
$SNR_T = \sigma_s^2 / \sigma_w^2$	13 dB	$l_{ref} = 1$ m
Noise Variance σ_w^2	1	Normalized
Reference Frequency	2.5 kHz	(Eckert et al., 1993), used for AAF
Temperature	3.8 °C	(Institute of Marine Research, 2020), used for AAF
Salinity	3.5 ‰	(Institute of Marine Research, 2020), used for AAF
Depth	350 m	(Bjørnbom, 2011), used for AAF
pH	8	(Vetrov and Romankevich, 2004), used for AAF
Spreading Coefficient k_{sc}	1.5	(Stojanovic, 2006)

7. Results

The values of $SNR_k = AAF^2(x_k, h_m) \cdot \sigma_s^2 / \sigma_w^2$ averaged among all hotspots show a mean attenuation of 90.28 % and are the following:

Table 2: Averaged Signal-to-Noise Ratio at the sensors

Sensor 1	Sensor 2	Sensor 3
2.4 dB	3.4 dB	1.4 dB

At sensor-level (Table 3 and Figure 3), the optimization of J results in local thresholds with values distant from those obtained optimizing ER or CZ which tend to be similar. When J is used, in fact, the thresholds are oriented towards smaller values of $P_{d,k}$ and $P_{f,k}$. The values of Area Under the Curve (AUC) of the averaged ROC curves among the three sensors have a standard deviation equal to $4 \cdot 10^{-3}$, this justifies the similar average performances among the sensors when tuned using the same objective function.

Table 3: Local threshold selection's results

Sensor	Value of Optimized Function	Threshold	$\overline{P_{d,k}}$	$\overline{P_{f,k}}$
1	$J = 0.1896$	1.6380	0.3902	0.2006
	$ER = 0.5886$	0.7919	0.5451	0.3735
	$CZ = 0.3417$	0.8427	0.5328	0.3586
2	$J = 0.2064$	1.7268	0.3952	0.1888
	$ER = 0.5785$	0.8271	0.5496	0.3631
	$CZ = 0.3504$	0.8896	0.5354	0.3456
3	$J = 0.1923$	1.5169	0.4104	0.2181
	$ER = 0.5845$	0.7947	0.5497	0.3727
	$CZ = 0.3450$	0.8435	0.5378	0.3584

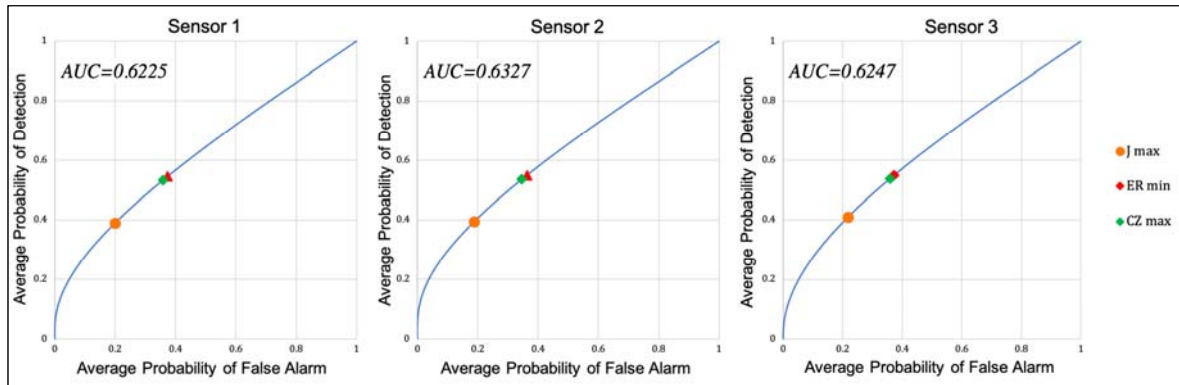


Figure 3: Averaged local ROC curves displaying the optimal points according to the different applied criteria

At FC-level, results were obtained with 10^8 Monte Carlo runs (Table 4 and Figure 4). The performance at a given threshold varies according to the objective function used for the sensors. When sensors are tuned using J , the optimal global threshold is divided between the value 1 if ER and CZ are optimized, and 2 if J is optimized. When sensors are tuned using ER or CZ , the optimal global threshold is always 2 using any optimization criterion. The highest value of AUC at the FC is obtained when sensors are tuned using J .

Table 4: Global threshold selection's results

Function used for Sensors	Value of Optimized Function	Threshold	$\overline{Q_d}$	$\overline{Q_f}$
Youden Index (J)	$J = 0.2546$	2	0.3608	0.1062
	$ER = 0.5553; CZ = 0.3774$	1	0.7442	0.4928
Closest-to-(0,1) (ER)	$J = 0.2562; ER = 0.5334; CZ = 0.3905$	2	0.5652	0.3090
Concordance Probability (CZ)	$J = 0.2598; ER = 0.5363; CZ = 0.3899$	2	0.5472	0.2875

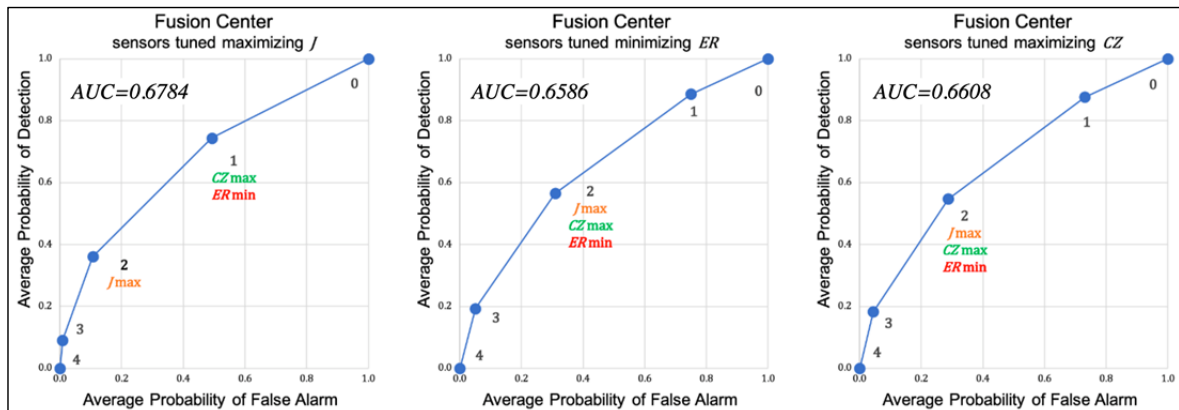


Figure 4: Averaged global ROC curves displaying the optimal points according to the different applied criteria

8. Conclusions

It is clear how the choice of the objective function at sensor-level is fundamental to determine the performances at FC-level for a given global threshold. The case study showed how tuning the sensors using the Youden Index increases the global AUC and orients the performances towards lower values of false alarm rate of the LDS, which may be preferable to avoid shutdowns. The optimal global thresholds show a similar behavior on the ROC space if compared to the results obtained when computing the optimal local thresholds. However, the tendency of the Youden Index to generate thresholds having a lower probability of detection and false alarm with respect to those generated by the other two indexes is less evident at FC-level since only $K + 2$ points can be placed on the ROC space. The three objective functions can also be adapted and corrected using coefficients to fit specific applications and requirements. The proposed methodology shows how important the number of sensors and their positioning can be and how the network performances heavily rely on the signal model. For this reason, more information regarding the statistical properties of the signal and other contributions that influence the AAF should be integrated if available. These factors can be signal perturbations, interferences, ambient noise, and oceanic phenomena (currents, tides, internal waves, etc.). This work is a step towards the integration of subsea monitoring using WSNs with Risk Assessment techniques necessary to localize the hotspots and to select the most appropriate objective function.

References

- Adegboye, M.A., Fung, W.K., Karnik, A., 2019. Recent Advances in Pipeline Monitoring and Oil Leakage Detection Technologies: Principles and Approaches. *Sensors* 19.
- Bai, Y., Bai, Q., 2012. *Subsea Engineering Handbook*, 1st ed. Gulf Professional Publishing, Houston, TX.
- Baroudi, U., Al-Roubaiey, A.A., Devendiran, A., 2019. Pipeline Leak Detection Systems and Data Fusion: A Survey. *IEEE Access* 7, 97426–97439.
- Bjørnbom, E., 2011. Goliat – Leak detection and monitoring from template to satellite. URL <https://www.norskoljeoggass.no/globalassets/dokumenter/drift/presentasjonerarrangementer/subsea-leak-detection--2011/4.-enino_n1862090_v1_eni_presentation_-_olf_seminar_-_subsea_leak_detection_-_03_november_2011.pdf> (accessed 6.6.20).
- Ciunozzo, D., Salvo Rossi, P., 2017. Distributed detection of a non-cooperative target via generalized locally-optimum approaches. *Inf. Fusion* 36, 261–274.
- Eckert, E.G., Maresca, J.W., Hillger, R.W., Yezzi, J.J., 1993. Location of Leaks in Pressurized Petroleum Pipelines by Means of Passive-Acoustic Sensing Methods, in: Durgin, P., Young, T. (Eds.), *Leak Detection for Underground Storage Tanks*. ASTM International, West Conshohocken, PA, pp. 53–69.
- Francois, R.E., Garrison, G.R., 1982a. Sound absorption based on ocean measurements: Part I: Pure water and magnesium sulfate contributions. *J. Acoust. Soc. Am.* 72, 896–907.
- Francois, R.E., Garrison, G.R., 1982b. Sound absorption based on ocean measurements. Part II: Boric acid contribution and equation for total absorption. *J. Acoust. Soc. Am.* 72, 1879–1890.
- Institute of Marine Research, 2020. Mareano. URL <<http://www.mareano.no/kart>> (accessed 6.6.20).
- Liu, X., 2012. Classification accuracy and cut point selection. *Stat. Med.* 31, 2676–2686.
- Paltrinieri, N., Comfort, L., Reniers, G., 2019a. Learning about risk: Machine learning for risk assessment. *Saf. Sci.* 118, 475–486.
- Paltrinieri, N., Landucci, G., Salvo Rossi, P., 2019b. An Integrated Approach to Support the Dynamic Risk Assessment of Complex Industrial Accidents. *Chem. Eng. Trans.* 77, 265–270.
- Paltrinieri, N., Scarponi, G.E., Khan, F., Hauge, S., 2014. Addressing dynamic risk in the petroleum industry by means of innovative analysis solutions. *Chem. Eng. Trans.* 36, 451–456.
- Røsby, E., 2011. Goliat development project - Subsea leak detection design. URL <https://www.norskoljeoggass.no/globalassets/dokumenter/drift/presentasjonerarrangementer/subsea-leak-detection--2011/15.-goliat-development-project_subsea_leak_detection_3_nov_2011_elling-rosby.pdf> (accessed 6.6.20).
- Shoari, A., Mateos, G., Seyed, A., 2016. Analysis of Target Localization With Ideal Binary Detectors via Likelihood Function Smoothing. *IEEE Signal Process. Lett.* 23, 737–741.
- Stojanovic, M., 2006. On the relationship between capacity and distance in an underwater acoustic communication channel, in: *Proceedings of the 1st ACM International Workshop on Underwater Networks - WUWNet '06*. ACM Press, New York, NY, pp. 41–47.
- Vetrov, A., Romankevich, E., 2004. *Carbon Cycle in the Russian Arctic Seas*, 1st ed. Springer, Berlin, Germany.
- Wong, G.S.K., Zhu, S., 1995. Speed of sound in seawater as a function of salinity, temperature, and pressure. *J. Acoust. Soc. Am.* 97, 1732–1736.